Performance Analysis of Vertical Sectorization in Sub-6-GHz Frequency Bands for 4G Mobile Network Under Realistic Deployment Scenario

Seifu Girma Zeleke(✉), Beneyam B. Haile, and Ephrem Teshale Bekele

Addis Ababa Institute of Technology, Addis Ababa University, Addis Ababa, Ethiopia
{seifu.girma,beneyamb.haile,ephrem.bekele}@aait.edu.et

Abstract. Demand for enhanced mobile broadband has been significantly increasing due to increasing penetration of data-intensive mobile services. For accommodating this demand, various network capacity enhancing technologies including cell densification and applying more frequency bands have been investigated and incorporated in the fourth generation (4G) and fifth generation (5G) mobile technologies. Network densification can be performed by either deploying new small cells or further sectoring horizontally and vertically existing network sites. Performance benefits of vertical sectorization have been investigated but mostly for theoretical network environment and user demand distribution that significantly affect the benefits. In this paper, we present performance analysis for vertical sectorization under realistic network environment and user distribution for selected urban area of Addis Ababa, Ethiopia. The analysis is performed for sub-6-GHz bands including those identified for 5G. Network simulation is performed using MATLAB while network modeling and assumptions are developed based on data collected for target area of Addis Ababa from network management system of the Addis Ababa network. Propagation is computed using deterministic 3D ray tracing method based on building map for the target area. Performance results show that considerable performance benefits are achieved by applying vertical sectorization for both cell edge and cell center users. For instance, we observe that 3×2 configuration presents 236.6%, 504% and 821.5% user throughput gains compared to 3×1 configuration at 10%-ile, 50%-ile and 90%-ile.

Keywords: Vertical sectorization · Sub-6-GHz bands · 4G · 5G · 3D ray tracing

1 Introduction

Demand for enhanced mobile broadband has been increasing and is predicted to increase significantly [1, 2]. According to ITU [2], mobile traffic will grow at an annual rate of around 55% in 2020–2030 and global mobile traffic per month is estimated to reach to 607 EB in 2025 and 5016 EB in 2030. The traffic growth is not only because of rise of subscriptions for mobile services but also grow in traffic volume consumed per user. The monthly average consumed traffic per user is predicted to be 39.4 GB and 257 GB in 2025

M. A. Delele et al. (Eds.): ICAST 2020, LNICST 384, pp. 231–243, 2021.
https://doi.org/10.1007/978-3-030-80621-7_17

and 2030, respectively [2]. Likewise, mobile traffic growth has also been observed in rising market like Ethiopia as a result of growth of mobile internet penetration and other multimedia service usage, particularly in the major cities like Addis Ababa, Ethiopia [3, 4].

Various capacity enhancing technological advancements are introduced aiming to support these continuous increasing mobile data demands [5]. The low, mid and high frequency bands have been exploited in addition to technological innovations to support the rising data demands [6–9]. Mobile network operators need to fulfill the data demand by upgrading their network via with these new technologies and frequency bands. Among the innovated technologies, network densification enhances system capacity by reusing frequency spectrum and limiting the coverage area [10]. Densification can be either macro with vertical sectorization or small cell densification. Small cell densification requires additional sites and associated network elements. Macro densification with vertical sectorization does not require additional sites; it requires antenna capability that splits the cells in to inner and outer cells (see Fig. 1). This reduces cost of sites and associated network elements.

However before deploying and using these enhanced mobile broadband their performance impacts in realistic network environment need to be investigated more.

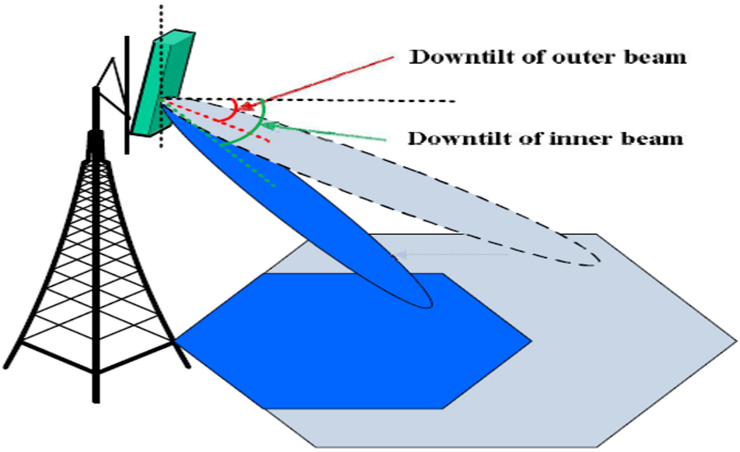

Fig. 1. Sector layout of vertical sectorization system [10].

A number of research works have been published regarding on vertical sectorization (VS). Early works mainly focus on study capacity impact of this technology for varying antenna configuration under synthetic simulation environments: propagation model, network layout, antenna pattern and demand nodes are simplified 3GPP cases [10–14]. The results showed promising gains can be obtained from this technique even if splitting the cell can introduce worse performance for cell edge users. Later optimization works which optimize network parameters with respect to antenna tilt angle, half power beam width and transmitted power of the method using different optimization techniques are conducted [15–19]. These later works also conducted simulation under synthetic environments. There are also some field trial experimental works that study and characterize the actual performance of vertical sectorization [20, 21]. Synthetic environment for simulation cases results in neglecting the influence of realistic network environments. However, there are very few works investigate the performance impact of this technology in realistic network environment [22–24] and work with the new operating frequency bands defined by 3GPP specification group [24].

The authors in [14] analyze the performance of different elevation beamforming scenarios: vertical sectorization with same carrier frequency, vertical sectorization with different carrier frequency based on CA and user-specific elevation beamforming. However, the paper conducted the research under legacy 2 GHz frequency band. Moreover, it works on the 3GPP simulation environments. Reference in [22] analyzed and compared performance impact of VS with super cell deployment and higher order horizontal sectorization in a real-world suburban environment. Reference in [23] examine performance impact of VS for various vertical HBPW and electrical tilt angles to observe the optimization space between two vertical sectors and the gain in terms of CDF of SINR and cell capacity. However, both references [22] and [23] do not consider the new operating bands. The author in [24] compare the performance of a cellular network using higher order sectorization in a horizontal domain, vertical sectorization, and super cell configuration under 28 GHz frequency as the operation band. However, it does not consider the sub 6 GHz frequency band. Moreover, it doesn't work on various combination of different inner and outer cell configuration. For best benefits of the technologies, their performances impact need to be investigated more under realistic network environments.

This research work addresses the aforementioned gaps stated above. Particularly, it investigates the performance impact of macro densification via vertical sectorization with the new operating subs-6 GHz frequency bands. These frequency bands are recommended to be used by both 4G and 5G network in addition to millimeter waves. Simulation is performed for various deployment scenarios focused to Addis Ababa use case. Realistic network environments imply: network topology of real building and terrain maps of Addis Ababa, Propagation is computed using deterministic 3D ray tracing and user distribution or demand nodes are located based on real network traffics collected from Ethio telecom.

The rest of paper is organized as follows: the next section presents system model and deployment scenarios. Studied scenarios, description of demand node distributions and parameters and assumptions used in simulation are described in Sect. 3. Section 4 provides simulation results and discussion. Finally, concluding discussions and potential research directions are given in Sect. 5.

2 System Model and Deployment Scenarios

2.1 System Model

This research work considers a downlink LTE mobile network with 18 numbers of macro sites in selected studied area as shown in Fig. 2. The notation c_m^i is used to refer macro LTE site having 3 sectors; each sector is identified by sector index i and m is used to show whether VS is applied or not at the i_{th} macro sector. For LTE macro sector, the value of m will be zero, but if VS is applied, m takes the value 1 and 2 to differentiate the inner and the outer sectors [25].

Without vertical sectorization, *SINR* of a user located at u is given by [25],

$$SINR = \frac{p\left(u, c_0^z\right)}{\sum_{i \neq z} p\left(u, c_0^i\right) + N} \tag{1}$$

Where, $p\left(u, c_0^z\right)$ is the received power of a user from serving sector c_0^z.

And the throughput (*TP*) performance, using Shannon formula is given by [26],

$$TP = BW_{eff} N_{PRB} B_{PRB} \ \log_2\left(1 + \frac{SINR}{SINR_{eff}}\right) \tag{2}$$

When VS is applied, *SINR* of a user located at u is given by,

$$SINR' = \begin{cases} \frac{p\left(u, c_1^z\right)}{\sum_{i \neq z}\left(\sum_{m=1}^{2} p\left(u, c_m^i\right)\right) + N}, \text{ when user is associated with outer sector} \\ \frac{p\left(u, c_2^z\right)}{\sum_{i \neq z}\left(\sum_{m=1}^{2} p\left(u, c_m^i\right)\right) + N}, \text{ when user is associated with inner sector} \end{cases} \tag{3}$$

Where, $p\left(u, c_1^z\right)$ and $p\left(u, c_2^z\right)$ are received signal powers of the user located at u from outer and inner sectors respectively.

And, the *TP* performance is given by,

$$TP' = BW_{eff} N_{PRB} B_{PRB} \ \log_2\left(1 + \frac{SINR'}{SINR_{eff}}\right) \tag{4}$$

Where, N_{PRB} is the number of Physical Resource Block (PRBs), B_{PRB} is the bandwidth per PRB, B_{Weff} is the adjusted bandwidth to fit with LTE system bandwidth efficiency and $\mathrm{SINR}_{\mathrm{eff}}$ is the adjusted SINR implementation efficiency.

The *TP* performance gain is then given by,

$$\eta = \frac{TP' - TP}{TP} \tag{5}$$

Antenna Models: In this paper, Huawei antenna patterns of the following models are used. For the existing 3 × 1 macro cells ADU451819 is used. In addition, AMAN software is used to create the required vertical and horizontal antenna pattern.

2.2 Deployment Scenarios

The analysis of vertical sectorization is performed for subs 6-GHz operating frequency bands specified by 3GPP specification groups and a down link LTE mobile network. The studied area is located in Addis Ababa Ethiopia that illustrates an urban scenario. The area is found around bole and covers an area of 2.82 km × 1.94 km. It has buildings of heights up to 80 m, terrain with different topography and latitude and longitudes of 38.745976 and 9.017116 respectively. The area consists of 18 macro cells; each site has 3 sectors in the existing Addis Ababa LTE network. The location of macro sites are shown below (see Fig. 2).

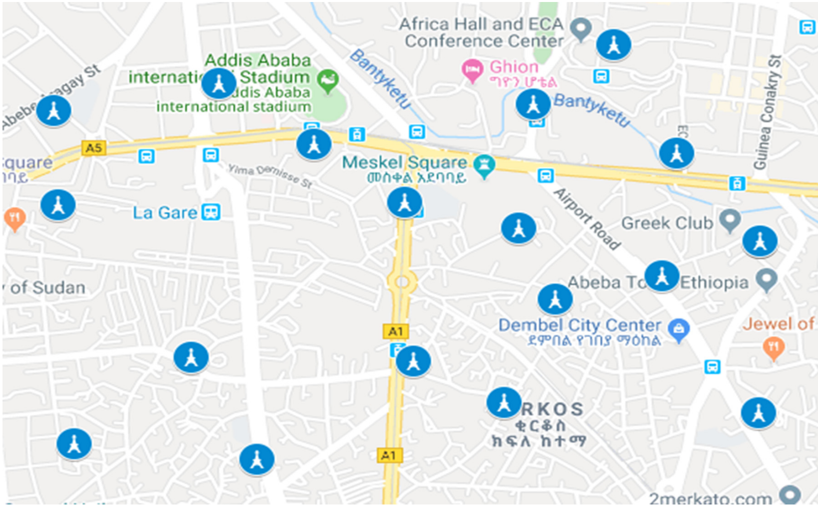

Fig. 2. Performance studied area.

3 User Distribution, Studied Scenarios and Simulation Setup

3.1 User Distribution

Demand nodes or user locations are one of the important parameters that has an impact on the performance of mobile network. Hence in this work, demand nodes are located using the real pick hour data collected from Ethio telecom.

To locate demand nodes, we did the following procedures. First, the studied area is divided in to several pixels. This is because the data are recorded pixel wise. The divided area has 10 rows and 14 columns. Then, for each pixel, we obtained the corresponding traffic density (g) and number of nodes (N). The traffic density is obtained dividing the collected traffic data of each pixel by the area of each pixel (a).

The number of demand nodes of each pixel is calculated as follows [27].

$$N_{\mathrm{m,n}} = \frac{a * g_{\mathrm{m,n}}}{r} \tag{6}$$

Where, a is the area of each pixel, $g_{\mathrm{m,n}}$ is the traffic density of each pixel and r is the individual data requirement which is assume equal for all and less than the minimum traffic density. The Generated user distribution is shown in Fig. 3 below.

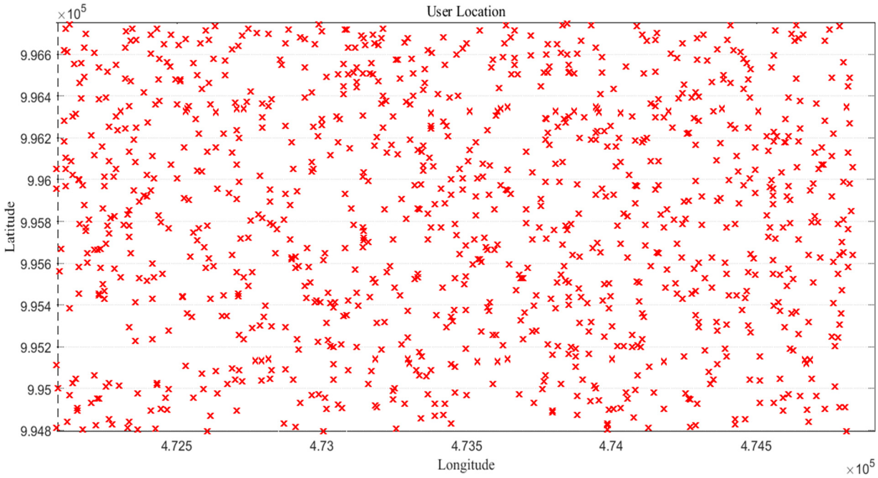

Fig. 3. Generated user demand nodes based on the above model.

3.2 Studied Scenarios and Simulation Parameters

Different scenarios are considered in this research work and they can be grouped in to two parts. The first group comprises scenarios 1 up to 4; both sectors use the same operating band. That means both inner and outer sectors configured with the same carrier frequency. The second group comprises scenarios 5 up to 7, different carrier frequencies are assigned to the inner and the outer sectors. Sectors configurations and simulation parameters and assumptions are shown in Table 1 and 2 below.

Table 1. Inner and outer sectors assigned frequency band.

Scenarios	Inner sector (MHz)	Outer sector (MHz)	Bandwidth (MHz)
Scenario 1	1800	1800	20
Scenario 2	2600	2600	80
Scenario 3	3600	3600	100
Scenario 4	5000	5000	100
Scenario 5	1800/2600	2600/1800	20/20
Scenario 6	1800/3600	3600/1800	(20/100)/20
Scenario 7	1800/5000	5000/1800	20/20

Table 2. Simulation parameters and assumptions.

Parameters	Values/Assumptions
Downlink transmit power	46 dBm
Frequency reuse factor	1
Base station height	40 m
Horizontal HPBW	64°
UE height	1.5 m
UE number in service area	1037
Simulation area	2.82×1.94 km^2
Receive antenna gain	0 dBi
BW_{eff}	0.5
$SINR_{eff}$	0.85
Thermal floor	−174 dBm/Hz
Noise figure	9 dB
Traffic distribution	Non-Uniform
Cell association	RSRP
Traffic model	Full buffer

4 Results and Discussions

This section presented performance of VS for LTE downlink mobile network with the new operating frequency bands defined by 3GPP group. Simulations are carried out to observe CDF of UE SINR and throughput performance of VS for different inner and outer band configuration stated in Sect. 3.2. All simulations are performed as follows: For each snapshot

- Pathloss of each user is calculated using proman
- Users are associated with their respective serving cell based on their signal level
- Assuming full load system, all available resource blocks are scheduled. Number of resource blocks for each user in a cell is the same.
- Calculate the down link SINR and throughput using Eq. (1), (2), (3) and (4) for all users.

Repeat this a number of times (400 times our case) and collect the statics.

Figure 4, 5 and 6 are plotted to see performance of UE SINR for network configuration categorized under group 1 and 2 which are listed in Table 1. What Fig. 4 makes different from Fig. 5 and 6 is that, the former use the same operating bands, whereas the latter uses different operating bands for inner and outer sectors. Figure 5 is plotted for the case which all the outer sectors use the legacy 1800 MHz bands and inner sectors are configured with the new frequency bands mentioned in Sect. 3.2. On the other hand,

Fig. 6 is plotted for the same inner carrier frequency 1800 MHz and different outer carrier frequency. For comparisons purpose the existing macro only (MO) 3 × 1 networks is used as a reference configuration.

As it can be seen in Fig. 4, applying vertical sectorization degrades CDF of UE SINR in all cases. This is because as a new cell incorporated, additional co-channel interferences also introduced. It can also be observed as the operating bands become higher CDF of UE SINR degrades more besides the more bandwidth we obtained. Among the studied cases, scenario 1 out performs the other studied configurations. But, as we move the lower operating bands, we get lower bandwidth as indicated in Table 1.

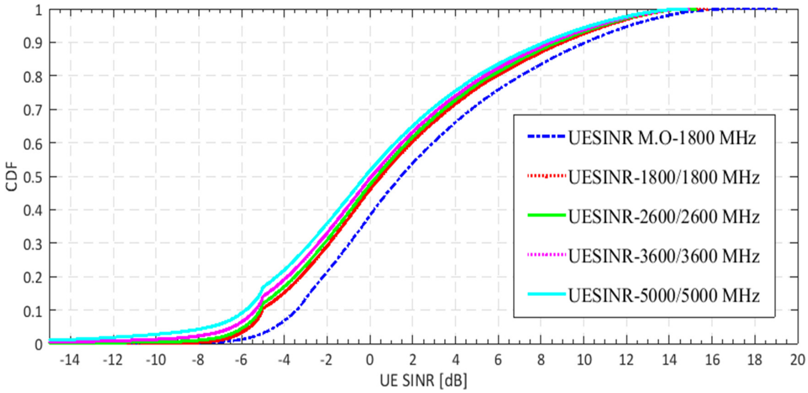

Fig. 4. CDF of UE SINR of the same inner and outer sectors bands configurations.

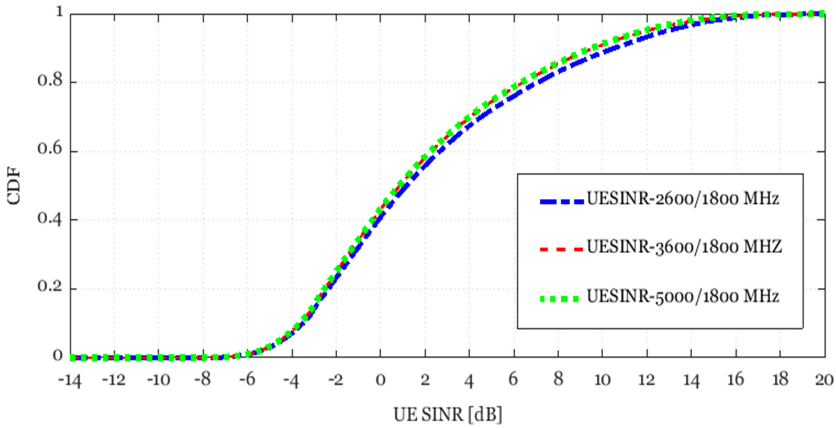

Fig. 5. CDF of UE SINR of the same outer sectors bands configurations.

Figure 5 and 6 are plotted to observe performance impact of configuring sectors with different operating frequency bands. As it can be seen in both figures such configuration has a better performance compared with sectors with same operating band. In Fig. 6, performance of the existing 3 × 1 configuration and group 2 cases are compared with respect to CDF of UE SINR under equal band width. As it can be observed from the figure, all configuration out performs the existing 3 × 1 MO configuration at 10%-ile, 50%-ile and 90%-ile of UE SINR (see Fig. 6).

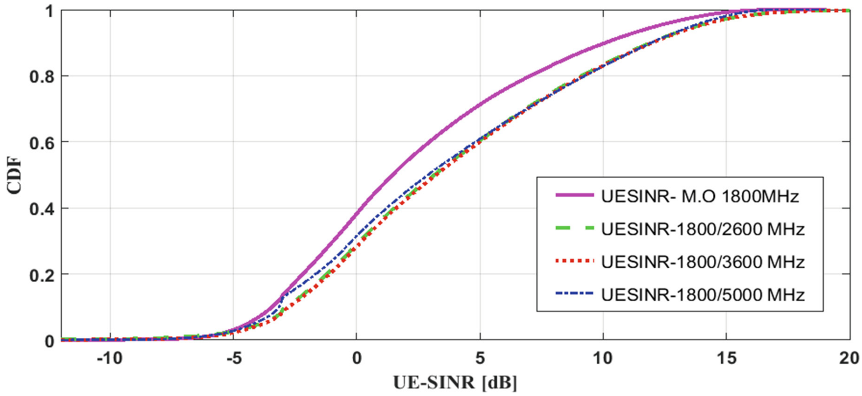

Fig. 6. CDF of UE SINR of the same inner sectors bands configurations.

Figure 7 is plotted to compare UE SINR of the existing MO network, VS 1800/1800 MHz and VS 1800/3600 MHz. Their UE SINR at 10%-ile: −3.44 dB, −5.04 dB and −2.76 dB, at 50%-ile: 1.46 dB, 0.51 dB and 3.24 dB and at 90%-ile: 10.12 dB, 8.96 dB and 11.99 dB respectively. The values show that scenario 6 out performs the other configuration at all percentile.

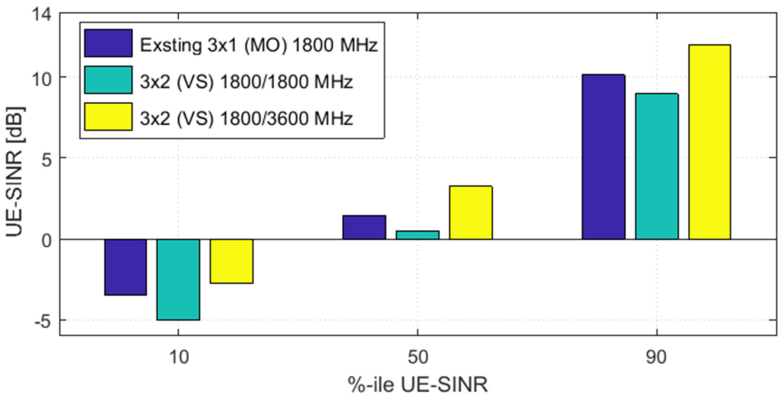

Fig. 7. Comparison of CDF of UE-SINR at 10%-ile, 50%-ile and 90%-ile.

Figure 8 and 9 show performance of UE throughputs which are plotted with antenna configuration listed under Table 1. The results are compared with the existing 3 × 1 network. As it can be observed in the figure, the entire identified configuration outperforms the existing 3 × 1 macro configuration. Specifically, scenario 6 significantly improves the performance of UE throughput in all percentiles.

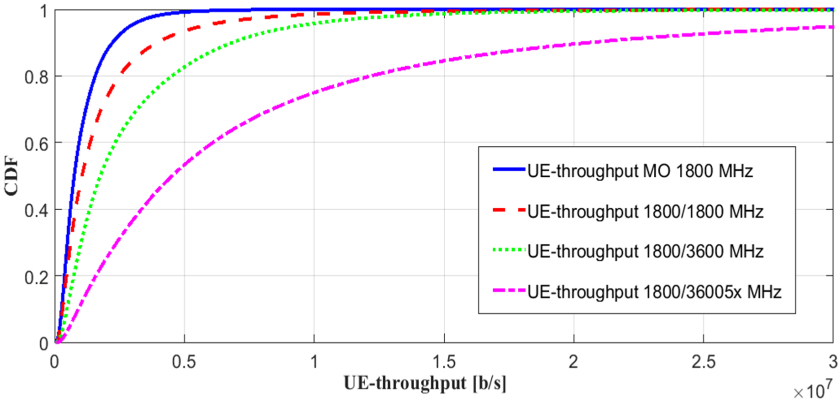

Fig. 8. CDF of UE throughput.

At 10%-ile UE throughput of the existing 3 × 1 configuration is about 0.273 Mbps where as scenario 6 with the same bandwidth is about 0.296 Mbps and scenario 6 with different band width is about 0.478 Mbps. At 50%-ile UE throughput of the existing 3 × 1 configuration is about 0.75 Mbps where as scenario 6 with the same bandwidth is about 1.06 Mbps and scenario 6 with different bandwidth is about 1.76 Mbps. At 90%-ile UE throughput of the existing network is about 2.23 Mbps whereas scenario 6 with same band width is about 3.96 Mbps and scenario 6 with the different bandwidth is about 6.83 Mbps (see Fig. 8 and 9).

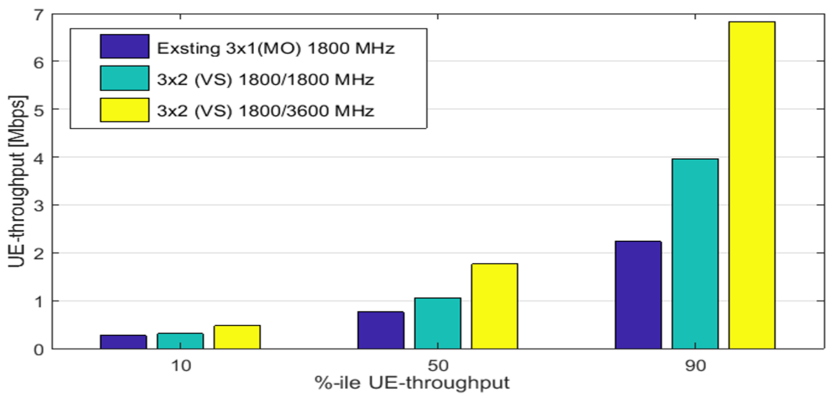

Fig. 9. Comparison of CDF of UE throughput at 10%-ile, 50%-ile and 90%-ile.

UE throughput gain at 10%-ile, 50%-ile and 90%-ile, for 3 × 2 1800/3600 MHz and 3 × 2, 1800/36005x MHz cases are compared to the existing 3 × 1 macro only configuration as depicted in Fig. 10. For equal bandwidth case, a relative gain of about 75.1%, 134.6% and 206.3 at 10%-ile, 50%-ile and 90%-ile respectively are obtained. For the case of 1800/36005x a gain of 236.6%, 504% and 821.5.7% at 10%-ile, 50%-ile and 90%-ile respectively are obtained compared with the existing macro only configuration (see Fig. 10). Therefore, applying vertical sectorization with different operating bands significantly improves both CDF of UE SINR and throughput at all percentile.

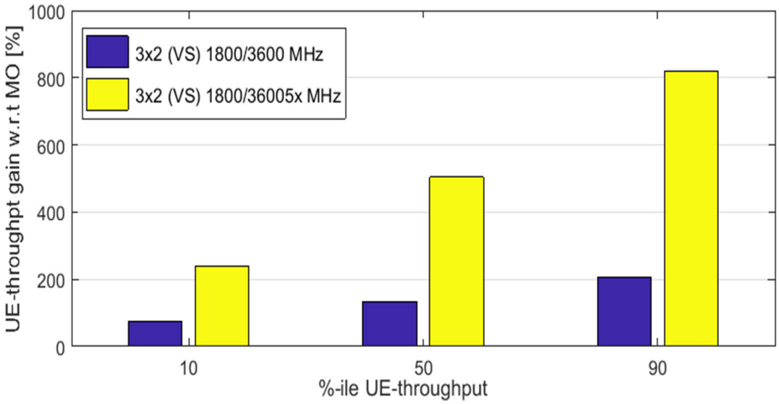

Fig. 10. UE-throughput percentile gain.

5 Conclusion

In this paper, we have analyzed performance impact of vertical sectorization in realistic network environment of Addis Ababa city for sub-6-GHz bands including the new 5G bands defined by 3GPP specification groups. CDF of UE SINR and throughput performances are used as a performance metrics. After analyzing the studied scenarios, throughput performance of the selected scenario is compared with the existing 3×1 LTE network. Based on the results, configuring VS with different operating bands results in a better performance compared to configuring both inner and outer sectors with the same carrier frequency. We also observed that, when the operating frequency become higher and higher UE SINR degrades. The identified configuration enhances system performance of user throughput up to 236.6%, 504% and 821.5% at 10%-ile, 50%-ile and 90%-ile respectively compared to the existing 3×1 configuration. This performance gain is obtained due to the introduction of additional resource elements and the improved UE SINR. Effect of vertical sectorization in high rise building, higher order vertical sectorization, multi objective optimization and cell association in vertical sectorization can be an important future work.

References

1. Cisco white paper, Cisco Visual Networking Index: Forecast and Methodology, 2016–2021. Cisco public (2017)
2. Report, IMT Traffic estimates for the years 2020 to 2030, ITU-R M.2370-0 (2015)
3. Adam, L.: Understanding what is happening in ICT in Ethiopia. A supply and demand side analysis of the ICT sector, Evidence for ICT Policy, Action Policy Paper (2012)

4. Haile, B.B., Aga, D., Mulu, B.: On the relevance of capacity enhancing 5G technologies for Ethiopia. In: 10th Ethiopian ICT Annual Conference, Addis Ababa, Ethiopia (2017)
5. Whitepaper, 5G vision and requirements, IMT-2020 (5G) Promotion Group (2015)
6. GSMA, 5G Spectrum: GSMA public policy position (2018)
7. Busari, S., Mumtaz, S., Al-Rubaye, S., Rodriguez, J.: 5G millimeter-wave mobile broadband: performance and challenges. IEEE Commun. Mag. **56**, 137–143 (2018)
8. 3GPP, 5G NR User Equipment (UE) radio transmission and reception, TS 38.101-1, Technical Specification, version 15.3.0 Release 15 (2018)
9. Sanad, M., Hassan, N.: A Sub-6 GHz multi-beam base station antenna for 5G with an arbitrary beam-tilting for each beam. In: Radio and Wireless Symposium (RWS), Orlando. IEEE (2019)
10. Fangchao, Z., et al.: A system level evaluation of vertical sectorization for active antenna system. In: 2015 IEEE/CIC International Conference on Communications, China, pp. 126–131. IEEE (2015)
11. Osman, N., Yilmaz, S., Jyri, H.: System level analysis of vertical sectorization for 3GPP LTE. In: 6th International Symposium on Wireless Communication Systems, Tuscany, pp. 453–457. IEEE (2009)
12. Youqi, F., Jian, W., Zhuyan, Z., Liyun, D., Hongwen, Y.: Analysis of vertical sectorization for HSPA on a system level: capacity and coverage. In: IEEE Vehicular Technology Conference (VTC Fall), Quebec, pp. 1–5. IEEE (2012)
13. Caretti, M., Crozzoli, M., Del, G., Orlando, A.: Cell splitting based on active antennas: performance assessment for LTE system. In: WAMICON 2012 IEEE Wireless & Microwave Technology Conference, Florida, pp. 1–5. IEEE (2012)
14. Song, Y., Yun, X., Nagata, S., Chen, L.: Investigation on elevation beamforming for future LTE-advanced. In: IEEE International Conference on Communications Workshop (ICC), Hungary (2013)
15. Wei, Z., Wang, Y., Lin, W.: Optimization of down tilts adjustment combining joint transmission and 3D beamforming in 3D MIMO. In: IEEE/CIC ICCC 2014 Symposium on Wireless Communications Systems, Shanghai, pp. 728–732. IEEE (2015)
16. Siew, N., Zhong, L., Sai, W., Yong, C.: Optimizing radio network parameters for vertical sectorization via Taguchi's method. IEEE Trans. Veh. Technol. **65**, 860–869 (2015)
17. Joydeep, A., Salam, A.: Optimizing vertical sectorization for high-rises. In: International Conference on Computing, Networking and Communications (ICNC), Garden Grove, pp. 1–5. IEEE (2015)
18. Jinping, N., Geoffrey, Y., Li, F., Wei, W., Weike, N., Xun, L.: Downtilts optimization and power allocation for vertical sectorization in AAS-based LTE-a downlink systems. In: IEEE 86th Vehicular Technology Conference (VTC-Fall), Toronto, pp. 1–5. IEEE (2017)
19. Fan, J., Li, W., Zhang, Y., Deng, J.: Fractional pilot reuse with vertical sectorization in massive MIMO systems. In: 2017 IEEE 85th Vehicular Technology Conference (VTC Spring), Sydney, pp. 4–7. IEEE (2017)
20. Fengyi, Y., Jianmin, Z., Weiliang, X., Xuetian, Z.: Field trial results for vertical sectorization in LTE network using active antenna system. In: IEEE International Conference on Communications (ICC), Sydney, pp. 2508–2512. IEEE (2014)
21. Weiliang, X., Qimei, C., Fengyi, Y., Qi, B., Yifei, Y.: Experimental investigation on a vertical sectorization system with active antenna. IEEE Commun. Mag. **54**, 89–97 (2016)
22. Muhammad, H., Usman, S., Jukka, L.: Analysis of vertical and horizontal sectorization in suburban environment using 3D ray tracing. In: 23rd International Conference on Telecommunications (ICT), Thessaloniki, pp. 1–6. IEEE (2016)
23. Zeleke, S., Haile, B.: Performance analysis of vertical sectorization for LTE realistic deployment scenario. In: Mekuria, F., Nigussie, E., Tegegne, T. (eds.) ICT4DA 2019. CCIS, vol. 1026, pp. 154–163. Springer, Cham (2019). https://doi.org/10.1007/978-3-030-26630-1_13

24. Usman, M., Ruttik, K., Jäntti, R.: Performance analysis of vertical and higher order sectorization in urban environment at 28 GHz. In: 26th International Conference on Telecommunications (ICT), Hanoi, pp. 8–10. IEEE (2019)
25. Derege, K., Wegmann, B., Viering, I., Klein, A.: Mathematical model for vertical sectorization (VS) in AAS based LTE deployment. In: 11th International Symposium Wireless Communication Systems, Barcelona, pp. 100–105. IEEE (2014)
26. Preben, M., et al.: LTE system capacity compared to Shannon bounds. In: IEEE VTC Spring 2007, Dublin, pp. 1234–1238. IEEE (2007)
27. Dongheon, L., Sheng, S., Xiaofeng, Z., Zhisheng, N.: Spatial modeling of the traffic density in cellular networks. IEEE Wirel. Commun. **21**, 80–88 (2014)